IDH1 regulates human erythropoiesis by eliciting chromatin state reprogramming

Mengjia Li[1,2,#], Hengchao Zhang[1,#], Xiuyun Wu[1,#], Mengqi Yu[1], Qianqian Yang[1], Lei Sun[1], Wei Li[2], Zhongxing Jiang[2], Fumin Xue[3], Ting Wang[1,*], Xiuli An[4,*], Lixiang Chen[1,*]

[1]School of Life Sciences, Zhengzhou University, Science Road 100, Zhengzhou, China 450001; [2]Department of Hematology, First Affiliated Hospital of Zhengzhou University, No.1 Jianshe East Road, Zhengzhou, China 450052; [3]Department of Gastroenterology, Childrens Hospital affiliated to Zhengzhou University, Zhengzhou, China 450000; [4]Laboratory of Membrane Biology, New York Blood Center, 310 East, 67th Street, New York, NY 10065.

# These authors contributed equally to this work.

* Correspond to: tingwang@zzu.edu.cn (Ting Wang); xan@nybc.org (Xiuli An); lxchen@zzu.edu.cn (Lixiang Chen)

Running heads: Roles of nuclear IDH1 in erythropoiesis regulation

Key Points:

1) IDH1 deficiency impaired terminal erythropoiesis;

2) IDH1 deficiency leads to chromatin states reprogramming by causing aberrant accumulation and genome-wide re-distribution of H3K79me3;

3) Dyserythropoiesis is caused by upregulation of SIRT1 induced by H3K79me3 accumulation.

Graphical Abstract

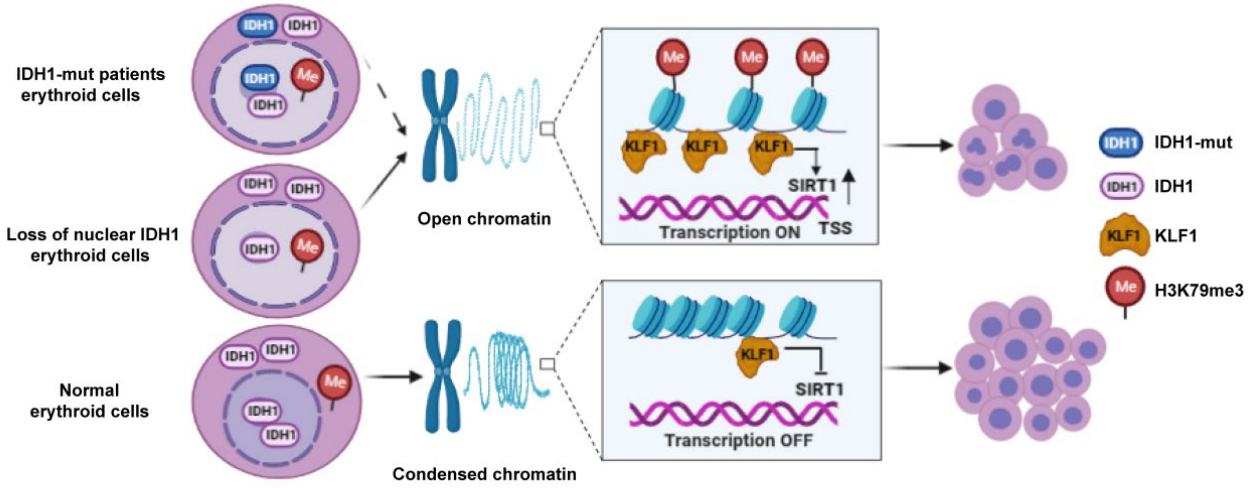

ABSTRACT

Isocitrate dehydrogenase 1 (IDH1) is the key enzyme that was involved in the modulation of cellular metabolism, epigenetic modification and redox states homeostasis. Gain-of-function mutations and decreased expression of IDH1 have been demonstrated to be tightly associated with the pathogenesis of various myeloid malignancies characterized by ineffective erythropoiesis, such as acute myeloid leukemia (AML) and myelodysplastic syndrome (MDS). However, the function and mechanism of IDH1 in human erythropoiesis still remains to be further explored. Here, utilizing the human erythropoiesis system, we present an evidence of IDH1-mediated chromatin state reprogramming besides its well-characterized metabolism effects. We showed that knockdown of IDH1 induced chromatin reorganization and subsequently led to abnormalities of various key biological events in erythroid precursors, which could not be rescued by addition of reactive oxygen species (ROS) scavengers or supplementation of α-ketoglutarate (α-KG). We further revealed that deficiency of IDH1 induces genome-wide changes in distribution and intensity of multiple histone marks, among which H3K79me3 was identified as a critical factor in chromatin state reprogramming. Integrated analysis of ChIP-seq, ATAC-seq and RNA-seq recognized that SIRT1 was the key gene affected by IDH1 deficiency. Thus, our current work provided novel insights for further clarifying fundamental biological function of IDH1 which has substantial implications for an in-depth understanding of pathogenesis of diseases with IDH1 dysfunction and accordingly development of therapeutic strategies.

Key words: IDH1; chromatin states; human erythropoiesis; H3K79me3

Introduction

Isocitrate dehydrogenase 1 (IDH1) is a key enzyme involved in regulation of redox homeostasis by catalyzing oxidative decarboxylation of isocitrate to α-ketoglutarate (α-KG), also known as 2-oxoglutarate (2-OG), simultaneously reducing $NAD(P)^+$ to NAD(P)H and liberating CO [1]. Growing evidence suggests that, in addition to metabolism regulation, IDH1 is also involved in regulation of epigenetic landscape[2]. IDH1 mutations are known to cause dysregulation of chromatin modifications, such as DNA methylation, histone acetylation and methylation, which are associated with the occurrence and development of various myeloid malignancies characterized by ineffective erythropoiesis, such as acute myeloid leukemia (AML) and myelodysplastic syndromes (MDS) [3,4]. Notably, recent research work also revealed that decreased expression of IDH1 are also contributed to the onset of AML and MDS [5,6].

Previous studies found that IDH1 mutations led to loss of normal catalytic activity [7] and gain of function, causing accumulation of the rare metabolite 2-hydroxyglutarate (2-HG) [8,9]. 2-HG acts as an "oncometabolite" by competitively inhibiting multiple α-KG-dependent dioxygenases[10-12], consequently altering cells epigenetic state and leading to pathogenesis of myeloid malignancies [1,9]. However, several recent studies have shown that suppression of mutant IDH1 expression and/or inhibition of 2-HG production is not sufficient to reverse mutant IDH1-induced epigenetic changes [13,14]. Blocking production of 2-HG did not inhibit the growth of many solid cancers with IDH1 mutations [13]. Importantly, although IDH1 mutations lead to gradual accumulation of DNA and histone methylation markers, inhibition of IDH1 mutation expression did not lead to complete restoration of epigenome and transcriptome to initial state [14]. Moreover, it has been reported that high concentration of 2-HG produced by mutant IDH1 also has antineoplastic activity in glioma [15]. All these findings strongly suggested that the roles of IDH1 mutations in the pathogenesis of AML and MDS might not only be attributed to its capability to produce 2-HG.

Considering that genetic mutations may lead to the loss of original functions while acquiring new roles, we speculate that the roles of IDH1 mutations in the pathogenesis of myeloid disorder diseases might not only be attributed to the gain of function-dependent manner, but also attributed to loss of function manner, which has not been recognized previously. It also should be noted that most previous studies focused primarily on the pathogenic roles of mutated IDH1, whereas the biological function of IDH1 and underlying mechanisms remain largely unknown.

In this study, by using an *in vitro* human erythropoiesis system, during which cell morphology and chromatin architecture are dramatically altered [16, 17], we presented an evidence that nuclear IDH1 is involved in chromatin state reprogramming to regulate terminal erythropoiesis.

Methods

Culture of CD34$^+$ cells and shRNA or siRNA mediated knockdown of IDH1. Primary human CD34$^+$ cells were acquired from cord blood by positive selection using CD34$^+$ magnetic selective beads system according to the manufacturers protocol [18]. The detailed methods have been described previously including culture medium composition, the culture protocol, preparation of lentivirus [19]. The sequence of IDH1-shRNA and IDH1-siRNA in experiments were shown in Supplemental Table 2.

Drug treatment. The drugs for cell treatment were as follows. N-Acetyl-L-cysteine (MCE, HY-B0215) used at a final concentration of 10μM. Glutathione (Selleck Chemicals, S4606) was dissolved in DMSO, and used at a final concentration of 50μM. α-ketoglutanic acid (MilliporeSigma, K1128) was used at a final concentration of 50μM. EX527 (Selleck, S1541) used at final concentrations of 10 and 200 nM and SRT1720 (MCE, HY10532) used at final concentrations of 0.1, 0.5 nM and 2.5μM.

Immunofluorescent staining of AML or MDS patients Paraffin-Embedded bone marrow cells. Formalin-fixed, paraffin-embedded tissues blocks of bone marrow samples from AML and MDS patients bearing IDH1 mutation were sectioned at a thickness of about 4-5 μm. Slides were floated in a 40°C water bath and then transferred onto glass slides. After drying for 12 hours, slides were deparaffinized with xylene and rehydrated with alcohol. Then, slides were incubated in 10 mM citrate buffer (pH 6.0) at 95-100°C for 10 minutes. 3% BSA in PBS were added onto slides and incubated at 25°C for 30 minutes. Slides were incubated with primary antibodies at 4°C for 12 hours and with secondary antibody at 25°C for 30 minutes. Nuclear was stained with Hoechst 33342 (blue). The following primary antibodies were used as follows: rabbit polyclonal antibody to IDH1(#12332-1-AP, Proteintech), mouse monoclonal antibody to Histone H3 (Tri methyl K79) (BSM-33098M, Thermo Fisher Scientific). Secondary antibodies were goat anti-rabbit or goat anti-mouse labeled with Alexa Fluor 488 or Cy5(Servicebio). Pannoramic MIDI (3DHISTECH) slice scanner was used to acquire images.

DNA pull-down assay. The sequence of the biotin labeled probes for SIRT1 was as follows (Forward oligo: TCCCAAAGTGCTGGGATTACAG; Reverse oligo: GCACCTCGGTACCCAATCG).

Genomic DNA containing the target DNA sequence was used as a template, the promoter region of SIRT1 was amplified by PCR, including biotin-labeled and non-biotin-labeled. 2ug probes (target gene biotin-labeled probe set and non-labeled probe set, Empty magnetic beads group) were added in EP tube and incubated for 8 hours in a 4°C refrigerator. 300 μL cell lysates (empty beads group without lysis solution) were added into magnetic bead-probe mixture and incubated in a 4°C refrigerator for 12 hours, 30μL (10%) of the remaining lysates were taken as the input group. Incubation mixture was centrifuged at 3000rpm for 2 minutes and washed 5 times. Loading buffer was added into each group (including input group and beads group). Tubes were input into boiling water bath for 10 minutes and centrifuged at 3000rpm for 5 minutes. The obtained production can be directly used for WB experiment.

Data analysis. We performed chromatin immunoprecipitation (ChIP)-seq, ATAC-seq and RNA-seq, detailed description of data analysis was provided in supplemental Data.

Results

IDH1 deficiency impaired terminal erythropoiesis.

Erythropoiesis is a continuous and complex process, it can be divided into two stages: early erythroid development and terminal erythroid differentiation.To further explore the roles of IDH1 during human erythropoiesis, we first analyzed the expression level of IDH1 from the transcriptomics data of highly purified populations of erythroid cells from cord blood at distinct stages of erythropoiesis. As shown in Supplemental Figure 1A, the expression of IDH1 was low in hematopoietic stem cells, but high in erythroid progenitor cells and late erythrocytes erythropoiesis. We collected cells at days 7, 9, 11, 13, and 15 during the process of erythroid differentiation and detected the mRNA and protein level of IDH1. As shown in Supplemental Figure 1B, C and D), IDH1 was consistently expressed at all stages of erythroid development. Then, we performed shRNA/siRNA-mediated knockdown of IDH1 on days 7, 11, and 15. ShRNA and siRNA mediated knockdown efficiency were confirmed by qRT-PCR (Supplemental Figure 2A) and western blot (Supplemental Figure 2B, C and Supplemental Figure 3A, B). Consistent with our previous results, we found that loss of IDH1 had a slight effect on cell growth (Supplemental Figure 2D) but not on apoptosis at late stages of erythropoiesis (Supplemental Figure 2E, F and Supplemental Figure 3C, D). Although the differentiation of colony-forming unit-erythroid (CFU-E) cells into terminal stage, characterized by glycoprotein A expression, was not affected by lack of IDH1 (Supplemental Figure

3E, F and Supplemental Figure 4A, B), the generation of orthochromatic cells, defined as GPA^{pos}α4-integrin^{low}band3^{hi} [21], was delayed by IDH1 deficiency (Supplemental Figure 4C, D and Supplemental Figure 5A, B). This delay of differentiation was also confirmed by morphological observation using cytospin assay (Supplemental Figure 4E). Since chromatin condensation and enucleation are distinguished cellular events of polychromatic and orthochromatic cells [21], we also evaluated cell morphology and enucleation. Based on the cytospins, both binucleated and multi-nucleated cells were both regarded as a nuclear malformation. There were at least 300 cells in each group, of which the number of abnormal nuclei cells as a percentage of the total number of cells was the proportion of aberrant nuclei， we observed a remarkable accumulation of polychromatic and orthochromatic erythroblasts with abnormal nuclei in IDH1-deficient erythroblasts (Figure 1A; Supplemental Figure 5C, D) and severely impaired enucleation (Figure 1B; Supplemental Figure 5E, F). In addition, we found that IDH1 deletion resulted in distinctly larger nuclei compared to controls, with the ratio of nucleus/plasma increased more than 2-fold in IDH1-deficient erythroid cells (Supplemental Figure 6A, B), indicating that IDH1 knockdown impaired nuclear condensation.

IDH1, a critical modulator of redox homeostasis and metabolism, catalyzes the conversion of isocitrate into α-KG in metabolism[13]. We have recently reported that IDH1 can regulate terminal stage human erythropoiesis by interacting with vitamin C [22, 23]. Interestingly, former study revealed that defect in erythropoiesis caused by IDH1 deficiency could not be rescued by reactive oxygen species (ROS) scavenging or α-KG supplementation, which indicates that IDH1 might perform its function partially in an enzyme-independent manner. To gain a better understanding of mechanism underlying effects of IDH1, we detected ROS and α-KG production. Firstly, we measured ROS production by flow cytometry using DCFHDA dye for quantitative and qualitative assessment of ROS based on the mean fluorescence intensity (MFI) of GFP. Results showed that MFI in IDH1-deficient group increased about 2-fold on day 15 (Supplemental Figure 7A). Although aberrant upregulation of ROS could be attenuated using ROS scavengers N-acetyl-L-cysteine (NAC, 10μM) and glutathione (GSH, 50μM) (Supplemental Figure 7B, C), generation of erythroblasts with abnormal nuclei or reduction of enucleation efficiency caused by IDH1 deficiency was not rescued (Figure 1C, D). In addition, we conducted colorimetric detection assay to determine α-KG levels [24], and found that lack of IDH1 resulted in a significant decrease in α-KG levels to 20nmol compared to 35nmol in control group on day 15 (Supplemental Figure 7D). However, supplementation with 50μM of α-KG could not rescue

aberrant cell events induced by lack of IDH1 (Supplemental Figure 7E; Figure 1E, F). These findings confirmed that IDH1 plays a crucial role in regulation of terminal human erythropoiesis in non-canonical functions manner. In addition, IDH1 deficiency led to the generation of erythroid cells with abnormal nuclei and reduction of mature red blood cells, which is consistent with dyserythropoietic features in myelodysplastic syndrome (MDS) and acute myeloid leukemia (AML) with erythroid dysplasia.

IDH1 localizes to nucleus of human erythroid cells.

IDH1 has been widely studied as a key metabolic enzyme localized in cytoplasm or peroxisome. In recent years, it has also been reported that IDH1 localized in nucleoplasm and chromatin of embryonic stem cells (ESCs) [20]. However, the subcellular localization of IDH1 during human erythropoiesis still remain largely unknown. To address this, we systematically analyzed the subcellular location of IDH1 in erythroid cells at different time points on umbilical cord blood-derived $CD34^+$ cells induced to normal human terminal erythroid development. Immunofluorescence analysis revealed that IDH1 was localized both in the nucleus and cytoplasm as cells matured (Figure 2A, B). We also examined location of IDH1 in human umbilical cord blood-derived erythroid progenitor 2 (HUDEP-2), K562 and HEL cell lines and found that IDH1was also localized both in the nucleus and cytoplasm (Figure 2C and Supplemental Figure 8A, B). In addition, we obtained paraffin-embedded bone marrow samples from 10 patients with IDH1-mutant AML/MDS, including 4 MDS and 6 AML samples (Supplemental Table1). IDH1 mutation sites were reported in previous studies, including R132C, R132G, and R132H [2]. We further detected localization of IDH1 by immunofluorescence staining assay, IDH1 was also expressed in both nucleus and cytoplasm of erythroblasts characterized as GPA positive expression (Figure 2D and Supplemental Figure 8C). In contrast, IDH1 was exclusively localized in cytoplasm of 293T cell line (Figure 2E). Western blot analyses further confirmed nuclear location of IDH1 in erythroblast but not in 293T cells (Figure 2F). The unique subcellular localization pattern of IDH1 in erythroid cells suggests that it may play a role in erythropoiesis through non-canonical functions.

IDH1 maintain nuclear morphological on terminal erythropoiesis.

Previously, presence of IDH1 in nucleus has been mentioned [20], but it has not been specifically proven that the function of IDH1 relies on its nuclear localization. To further test the function of IDH1

in maintaining nucleus morphology, we knocked out IDH1 in nucleus while retaining cytoplasmic IDH1 (Figure 3A). Firstly, as shown in Figure 3B, we knocked out IDH1 using CRISPR-Cas9 technology by infecting with viral particles carrying small guide RNA (sgRNA) sequences targeting IDH1 and sorted with GFP to get Sg-IDH1 HUDEP2 cells, in which IDH1 was totally depleted. Cells overexpressing nuclear export signal (NES)-IDH1 were then transduced into Sg-IDH1 HUDEP2 to deplete nuclear IDH1 while preserving IDH1 in cytoplasm in HUDEP2 cells. After expansion and differentiation [25], we further confirmed the selective localization of IDH1 to nucleus by confocal microscopy. As shown in Figure 3C and D, there is no presence of IDH1 in nucleus while the cytoplasm localization of IDH1 was still retaining. Then, we further performed Edu staining to detect cell cycle by FACS, as shown in Figure 3E and F, we found that cell cycle arrest in G0/G1 and S phase in Sg-IDH1 and Sg-NES-IDH1 groups. Selective knockdown of nuclear IDH1 caused a significant increase of the proportion of HUDEP2 cells with abnormal nuclei (Figure 3G). While, as it was shown in Figure 3H, statistical analysis showed that proportion of cell nuclear malformations of Sg-NES-IDH1 cells was as similar as Sg-IDH1 cells. Taken together, these results demonstrated that nuclear IDH1 also plays critical roles in maintaining of nuclear morphology during terminal erythropoiesis.

Deficiency of IDH1 reshaped chromatin landscape in late-stage erythroblasts.

Given that nuclear located chromatin-binding proteins play crucial roles in maintaining chromatin structure and gene expression [26], we further checked the distribution of IDH1 in nucleus of erythroid cells cultivated on day 15. We found that IDH1 is detected in chromatin fraction of erythroid cells on day 15 (Figure 4A). To explore the role of IDH1 in maintaining chromatin architecture, we evaluated the effect of IDH1 on the chromatin structure of erythroid cells using transmission electron microscopy. As expected, IDH1 deficiency led to aberrant dynamic transition between euchromatin and heterochromatin state. In mixed late erythroblasts on day 15 as well as purified polychromatic and orthochromatic cells, the proportion of euchromatin increased by 2-3 folds in IDH1-deficient cells compared to control cells (Figure 4B, C). There is growing evidence that metabolites drive chromatin dynamics through post-translational modifications (PTMs) that alter chromatin structure and function [27, 28]. Moreover, it has been well established that dynamic changes in methylation and demethylation of histone proteins could modify their interaction with DNA, consequently changing the ratio of heterochromatin and euchromatin [29]. Thus, we next detected histone modification marks using immunofluorescence imaging and western blotting. For most histone modifications, such as

H3K36me2, H3K4me3, H3K4me2, and H3K36me3, there were no significant differences between IDH1-deficient groups and control group on day 15 (Supplemental Figure 10A, B). However, abundance and subcellular location of specific histone modifications altered dramatically, including H3K27me2, H3K79me3, and H3K9me3. In control group, the majority of histone modification markers were released to cytoplasm for final degradation. While in IDH1-deficient groups, H3K27me2, H3K79me3, and H3K9me3 were still arrested in nucleus (Figure 4D-F). Taken together, all these results strongly suggested that nuclear IDH1 played critical roles in maintaining chromatin state dynamics by affecting accumulation and distribution of specific histone modifications.

Identification of H3K79me3 as the critical factor in response to IDH1 deficiency

Previous studies have reported that mutant-IDH1 induced chromatin state altering and thus drive development of gliomas and other human malignancies. To further define chromatin state reprogramming induced by IDH1 deficiency during erythropoiesis, we used chromatin immunoprecipitation followed by ChIP-seq to investigate genome-wide distribution of three key histone modifications in IDH1-deficient groups on day 15. Firstly, heatmaps and corresponding profile plots of 3 replicates for ChIP-seq data showed that there was the greatest increase in recruitment of H3K79me3 to chromosome (Figure5A, B). In addition, there were 21,169 peaks of H3K79me3 identified, which were significantly larger than 91 peaks of H3K27me2 and 1740 peaks of H3K9me3 (Figure 5C). We further analyzed the peak localization of H3K79me3, H3K27me2, and H3K9me3. Around 45% peaks of H3K79me3 were located in promoter regions. While for H3K27me2 and H3K9me3, peaks covered a large proportion in the distal intergenic region, approximately ~70% (Figure 5D). In fact, there were 8602 peaks with H3K79me3 in promoter region, which was ~800-fold more than that of H3K27me2 and H3K9me3 (Figure 5E). We subsequently conducted Gene Ontology (GO) analysis on the differential peaks. GO terms from biological processes, cellular components, and molecular functions consistently showed that H3K79me3 peaks were predominantly enriched with promoters of genes involved in RNA splicing and chromatin modification pathway (Figure 5F). Taken together, these results indicated that IDH1 deficiency reshaped chromatin states by altering the abundance and distribution of H3K79me3, which was the mechanism underlying roles of IDH1 in modulation of terminal erythropoiesis.

We further detected location of H3K79me3 in control and Sg-NES-IDH1 HUDEP-2 cell line and found that deletion of nuclear IDH1 induced H3K79me3 accumulation in nucleus (Supplemental

Figure 11A). The production of erythrocytes with abnormal nuclei and the reduction of mature erythrocytes due to IDH1 deletion are prominent features of MDS and AML. In addition, pathogenesis of AML/MDS is significantly associated with IDH1 mutation [30]. Therefore, we speculated that aberrant accumulation and distribution of H3K79me3 caused by dysfunction of IDH1 were also another characteristic of MDS/AML bearing IDH1 mutation. Thus, we performed immunofluorescence microscopy observation to further investigate the clinical significance of H3K79me3 in progression of IDH1-mut AML/MDS (Supplemental Table 1). Notably, an interesting finding was that H3K79me3 colocalized with IDH1 mutants in nucleus (Supplemental Figure 11B）.

IDH1 deletion increased chromatin accessibility in late-stage erythroblasts

Histone modifications are important epigenetic markers involved in multiple cellular processes via regulation of gene transcription or remodeling of chromatin structure [31, 32]. Since previous studies have identified H3K79me3 as a transcriptional activating marker [33], we speculated that accumulation of H3K79me3 in IDH1-deficient erythroblasts would subsequently lead to switch of closed chromatin into open chromatin. To test our hypothesis, we performed Assay for Transposase-Accessible Chromatin with high-throughput sequencing (ATAC-Seq) to identify alterations in chromatin accessibility (Supplemental Figure 12A, B). Heatmaps and corresponding profile plots displayed chromatin accessibility of Luciferase-shRNA and IDH1-shRNA at peak centers. We found that IDH1-deficient cells showed higher ATAC peak signals compared to control cells (Figure 6A, B). Volcano plot showed that there were 2,637 ATAC peaks gained and 442 ATAC peaks lost in presence of IDH1 deficiency (Figure 6C). Analysis of localization of ATAC peaks showed that differential peaks were mainly located in promoter regions (Figure 6D; Supplemental Figure 12C). GO analysis showed that gained ATAC peaks were mainly enriched with promoters of genes involved in various chromatin regulation pathways (Figure 6E). To identify which specific DNA binding motifs were enriched in differential peaks, we performed motif analysis using HOMER and found that gained ATAC promoter peaks were enriched with KLF1 binding motifs ($p<0.001$), which was identified as an erythroid-specific transcription factor (Figure 6F). Therefore, these results further confirmed that nuclear IDH1 plays a critical role in chromatin structure modulation as determined by accumulation and distribution of H3K79me3.

Integrated analysis of ChIP-seq, ATAC-seq and RNA-seq identified SIRT1 as one of the key genes affected by IDH1 deficiency

To further elucidate mechanisms underlying effects of IDH1 deficiency on changes in chromatin landscape and transcriptional state, we conducted integration analysis of ChIP-seq, ATAC-seq and RNA-seq. RNA-seq analysis was performed to get widespread gene expression in control and IDH1-deficient erythroid cells (Supplemental Figure 13A). Volcano plot and heatmap of differentially expressed genes revealed that 3,543 genes were upregulated and 3,295 genes were downregulated after IDH1 knockdown (Supplemental Figure 13B-C, E). GO analysis showed that upregulated genes mainly enriched in pathway associated with chromatin, such as chromatin organization and chromatin remodeling (Supplemental Figure 13D). We further displayed chromatin-related genes, including *TSPYL1, SIRT1* and others (Supplemental Figure 12F). Further integrated analysis of RNA-seq and ChIP-seq showed that gene expression levels of H3K79me3-marked genes were upregulated in IDH1-deficient cells (Supplemental Figure 14A, B). Furthermore, integrated analysis of ChIP-seq and ATAC-seq confirmed that IDH1 loss resulted in a greater proportion of open chromatin regions in H3K79me3-enriched sites (Supplemental Figure 14C). Gene Set Enrichment Analysis (GSEA) showed that chromatin structure modulating pathway, including chromatin silencing and gene expression epigenetics (Figure 7A). We found that there were 93 genes overlap in ATAC-seq, ChIP-seq and RNA-seq (Figure 7B), of which 3 genes shared in chromatin-associated pathways, including *SIRT1, NUCKS1* and *KMT5A* (Figure 7C). Transcription factors (TFs) play key roles in regulation of transcription by recognizing and binding to target gene promoter region. Due to deficiency of IDH1, gained ATAC promoter peaks were enriched with KLF1 binding motifs (Figure 6F). IDH1 deficiency caused alteration of chromatin landscape, characterized by aberrant accumulation and distribution of H3K79me3, which led to dysregulation of terminal erythropoiesis. Thus, we speculated that H3K79me3 was involved in SIRT1 up-regulation. Representatively, gene expression levels and ATAC peak signals at SIRT1, *NUCKS1 and KMT5A*locus were elevated in IDH1-shRNA group and were accompanied by enrichment of H3K79me3 (Figure 7D). KLF1 has been characterized as one of the most significant TFs involved in regulation of human erythropoiesis. We thus detected TFs bound on *SIRT1, NUCKS1 and KMT5A* locus. ChIP-seq results showed that KLF1 could bind to promoter regions *SIRT1, NUCKS1 and KMT5A* with the highest peak signal at promoter of *SIRT1* (Figure 7E). Using DNA pull-down assay, we further confirmed that H3K79me3 binds to *SIRT1* gene promoter region in response to IDH1 knockdown (Figure 7F). These findings strongly suggested that IDH1 deletion can lead to increased accumulation of H3K79me3 in *SIRT1* promoter region and thus switch

region into open state, thereby recruiting KLF1 to promote *SIRT1* expression.

SIRT1 plays a critical role in mediating the regulatory effect of IDH1 during terminal stage erythropoiesis

Further integrated analysis also provided evidence to support our forementioned findings. As shown in Figure 7F, RNA-seq, ATAC-seq and ChIP-seq signal tracks annotated to SIRT1 gene loci showed H3K79me3/ATAC-seq overlap and corresponding upregulation of SIRT1 in IDH1 knockdown group. Based on these results, we speculated that SIRT1 was the key factor that mediated the role of IDH1 in regulation of terminal erythropoiesis. Therefore, we performed verification and rescue experiments by treatment of normal erythroid cells with a SIRT1 activator or treatment of IDH1-deficient cells with a SIRT1 inhibitor, respectively. First, we confirmed that the application of SRT1720 on normal erythroid cells and treatment of IDH1-deficient erythroid cells with SIRT1 inhibitor have no effect on terminal differentiation and did not induce apoptosis (Supplemental Figure 15 and 16). The addition of SRT1720 led to nuclear malformations in a dose-dependent manner, in approximately 40% of cells (Figure 8A). Importantly, we observed a significant enucleation reduction after addition of SRT1720. In control group, the percentage of enucleated cells was 30% and 45% on day 13 and day 15, respectively, compared to < 20% in SRT1720 group (Figure 8B). Therefore, SIRT1 activation mimicked the cell dysfunction caused by IDH1 knockdown. Morphological images of IDH1-deficient erythroid cells treated with EX527 showed that malformed nuclei were partially rescued (Figure 8C). In addition, treatment with SIRT1 inhibitor EX527 also partially increased enucleation efficiency to 25% and 35% on day 13 and day 15, respectively (Figure 8D). In conclusion, these findings prove that SIRT1 is a key regulatory factor that mediates roles of IDH1 in regulation of nuclear morphology and enucleation of terminal stage erythropoiesis.

Discussion

The effective diagnosis and treatment of tumors bearing IDH1 mutations relies on an understanding of the fundamental biological and physiological roles of IDH1. In this study, we delineated an enzyme activity-independent role of IDH1 in regulation of human erythropoiesis through remodeling chromatin state. We demonstrated that deficient nuclear IDH1 led to dramatic accumulation of multi-histone modifications, among which H3K79me3 was identified as the crucial

factor, resulting in SIRT1 upregulation and consequently leading to defects in various critical cell events during terminal stage erythropoiesis.

Recent advances in understanding non-catalytic activity of metabolism enzymes have provided insights into roles of IDH1 [34]. Change in subcellular distribution of metabolism enzymes is associated with distinct non-canonical functions. It has been reported that metabolic intermediates such as acetyl CoA, α-KG, S-adenosylmethionine, and nicotinamide adenine dinucleotide can act as cofactors of epigenetic modification of nuclear genes to regulate stem cell function and differentiation [35]. Interestingly, as a metabolic enzyme, hexokinase 2 (HK2) localizes to nucleus of AML and normal hematopoietic stem and progenitor cells, and nuclear HK2 has a non-canonical mechanism by which mitochondrial enzymes influence stem cell function independently of their metabolic function [34]. In addition, glycolytic enzymes that are translocated to nucleus have independent catalytic roles, such as kinase activity and DNA-binding ability that are associated with regulation of gene expression and DNA repair. For instance, nuclear translocated glyceraldehyde 3-phosphate dehydrogenase can bind to E3 ubiquitin ligase SIAH1 and initiate apoptosis, as well as bind to telomeres to maintain their length [36]. In this study, we found that IDH1, as one of key metabolism enzymes, localizes to nucleus in erythroid cells of healthy person and AML/MDS patients, and plays critical roles in maintaining cell morphology and chromatin dynamics in non-canonical functions manner.

Although a few studies have reported that IDH1 is located in nucleus, most studies have focused on the metabolism and RNA binding of IDH1 located in cytoplasm [20]. In line with previous findings, our study confirmed the critical role of IDH1 in regulation of human erythropoiesis, which could not be rescued by addition of ROS scavengers or supplementation with α-KG [22, 23]. Previous work reported that IDH1 regulate human erythropoiesis modulating metabolism, based on the finding that defective erythropoiesis induced by IDH1 deficiency could be reversed by application of vitamin C. It should be noted that Vitamin C is a critical metabolic regulator that plays important biological and physiological roles, as well as epigenetic modulatory roles, but underlying mechanism still remains to be well illustrated [37, 38]. Based on diverse outcomes of vitamin C treatment and metabolism restoration, we proposed that IDH1 might elicit its effect partially in an non-canonical functions.

Interestingly, we found that IDH1 deficiency had no obvious effect on differentiation and proliferation of proerythroblasts and basophils but affected unique cell events of polychromatic and orthochromatic erythroblasts, including cell morphology, chromatin condensation, and enucleation.

Terminal stage erythropoiesis is a highly dynamic and complex process during which chromatin structure undergoes significant changes [39]. Current and previous studies showed that in addition to chromatin condensation, majority of histones were released into cytoplasm for decomposition during late stage of terminal erythropoiesis and is crucial for chromatin condensation and subsequent enucleation [40]. Chromatin reorganization, histone release, and redistribution are essential for chromatin reprogramming on terminal erythroid development. In present study, our finding showed that IDH1 deficiency led to accumulation of multiple histone modification markers in nucleus, particularly in polychromatic and orthochromatic cells, might explain effects of IDH1 deficiency at specific development stages. In addition, we found that IDH1 deficiency caused methylated histones accumulation on chromatin and increased accessibility to generate open chromatin state for transcription activation, which further exacerbates defective terminal erythropoiesis. Present study is first to report that nuclear IDH1 has important roles in maintenance of dynamic changes in chromatin states. Our findings suggest synergistic actions of nuclear IDH1 and cytoplasmic on regulation of human erythropoiesis by modulating metabolism and chromatin architecture.

Our results also suggested that IDH1 deficiency was related to aberrant accumulation of H3K79me3 and SIRT1 upregulation. Although disturbed methylation catalyzed by DOT1 is a well-recognized target for diagnosis and treatment of leukemia and its transformation, the majority of previous studies mainly focused on the role of H3K79 demethylation [41-43]. In this study, in vitro and in vivo (patient samples) experiments showed that IDH1 deficiency led to significant H3K79me3 accumulation, which could be used to diagnose dyserythropoiesis with IDH1 functional defect. SIRT1 is important for catalyzing removal of acetyl groups from non-histone and histone proteins. Previous studies have demonstrated that SIRT1 is involved in a wide range of physiological functions, including regulation of gene expression, cell growth, DNA repair [44], oxidative stress [45], metabolism [46] and aging [47]. In addition, SIRT1 activates expression of fetal hemoglobin genes in adult human erythroblasts [48]. Notably, SIRT1 is also involved in regulation of higher-order chromatin structure and various pathways related to pathogenesis and transformation of various dyserythropoiesis-related hematopoietic diseases [49]. Overexpression and underexpression of SIRT1 are strongly associated with pathogenesis of AML and MDS. Both inhibitory and activatory strategies have been proposed for diagnosis and treatment of these diseases [50]. In current study, we proved that IDH1 deficiency leads to significantly increased SIRT1 expression. Series of phenotypes caused by IDH1 deficiency, such as

nuclear malformation, aberrant nuclear condensation, and impaired enucleation, could be partially rescued by addition of specific SIRT1 inhibitor. These findings confirm that inhibitory strategy is promising for diagnosis and treatment of dyserythropoiesis-related diseases, particularly in patients with IDH1 mutation.

In conclusion, our work provides a novel insight into the role of IDH1 in the regulation of chromatin states. The findings related to IDH1-H3K79me3-SIRT1 regulatory axis indicates that H3K79me3 and SIRT1 may be targeted for the diagnosis and treatment of diseases with IDH1 mutations.

Data availability.

The data underlying this article are available in article and in its online supplementary material. RNA-seq data have been deposited in the GEO under accession code GSE223141. ChIP-seq data have been deposited in the GEO under accession code GSE222296. ATAC-seq have been deposited in the GEO under accession code GSE222401.

Author contributions: X.A. and L.C. designed the overall project, analyzed the results and prepared the manuscript, with input from all co-authors. M.L. performed the experiments with assistance from M.Y., Q.Y. and L.S.; H.C.Z. and X.W. performed the integrated bioinformatics analysis under the supervision of T. W.; W.L., Z.J. and F.X. performed the analysis of the samples from patients bearing IDH1 mutation.

Acknowledgements: This work was supported by grants from the Natural Science Foundation of China (82170116, 81870094, 81570099 and 82300134).

Conflict of interest: The authors declare that they have no competing financial interests.

Reference

1. Waitkus MS, Diplas BH, Yan H. Biological Role and Therapeutic Potential of IDH Mutations in Cancer. Cancer Cell. 2018;34(2):186-195.
2. Chan SM, Thomas D, Corces-Zimmerman MR, et al. Isocitrate dehydrogenase 1 and 2 mutations induce BCL-2 dependence in acute myeloid leukemia. Nat Med. 2015;21(2):178-184.
3. Gbyli R, Song Y, Liu W, et al. In vivo anti-tumor effect of PARP inhibition in IDH1/2 mutant MDS/AML resistant to targeted inhibitors of mutant IDH1/2. Leukemia. 2022;36(5):1313-1323.
4. Liu ACH, Cathelin S, Yang Y, et al. Targeting STAT5 signaling overcomes resistance to IDH inhibitors in acute

myeloid leukemia through suppression of stemness. Cancer Res. 2022;82(23):4325-4339.
5. Liu ZY, Tian MY, Ding K, et al. High expression of PIM2 induces HSC proliferation in myelodysplastic syndromes via the IDH1/HIF1-α signaling pathway. Oncol Lett. 2019;17(6):5395-5402.
6. Yun S, Vincelette ND, Yu XQ, et al. TFEB links MYC signaling to epigenetic control of myeloid differentiation and acute myeloid leukemia. Blood Cancer Discov. 2021;2(2):162-185.
7. Yang H, Ye D, Guan KL, Xiong Y. IDH1 and IDH2 mutations in tumorigenesis: mechanistic insights and clinical perspectives. Clin Cancer Res. 2012;18(20):5562-5571.
8. Dang L, White DW, Gross S, et al. Cancer-associated IDH1 mutations produce 2-hydroxyglutarate. Nature. 2009;462(7274):739-744.
9. Gross S, Cairns RA, Minden MD, et al. Cancer-associated metabolite 2-hydroxyglutarate accumulates in acute myelogenous leukemia with isocitrate dehydrogenase 1 and 2 mutations. J Exp Med. 2010;207(2):339-344.
10. Ward PS, Patel J, Wise DR, et al. The common feature of leukemia-associated IDH1 and IDH2 mutations is a neomorphic enzyme activity converting alpha-ketoglutarate to 2-hydroxyglutarate. Cancer Cell. 2010;17(3):225-234.
11. Xu W, Yang H, Liu Y, et al. Oncometabolite 2-hydroxyglutarate is a competitive inhibitor of alpha-ketoglutarate-dependent dioxygenases. Cancer Cell. 2011;19(1):17-30.
12. Figueroa ME, Abdel-Wahab O, Lu C, et al. Leukemic IDH1 and IDH2 mutations result in a hypermethylation phenotype, disrupt TET2 function, and impair hematopoietic differentiation. Cancer Cell. 2010;18(6):553-567.
13. Tateishi K, Wakimoto H, Iafrate AJ, et al. Extreme Vulnerability of IDH1 Mutant Cancers to NAD+ Depletion. Cancer Cell. 2015;28(6):773-784.
14. Turcan S, Makarov V, Taranda J, et al. Mutant-IDH1-dependent chromatin state reprogramming, reversibility, and persistence. Nat Genet. 2018;50(1):62-72.
15. Su R, Dong L, Li C, et al. R-2HG Exhibits Anti-tumor Activity by Targeting FTO/m(6)A/MYC/CEBPA Signaling. Cell. 2018;172(1-2):90-105 e123.
16. Chen K, Liu J, Heck S, Chasis JA, An X, Mohandas N. Resolving the distinct stages in erythroid differentiation based on dynamic changes in membrane protein expression during erythropoiesis. Proc Natl Acad Sci U S A. 2009;106(41):17413-17418.
17. Baron MH, Barminko J. Chromatin Condensation and Enucleation in Red Blood Cells: An Open Question. Dev Cell. 2016;36(5):481-482.
18. Qu X, Zhang S, Wang S, et al. TET2 deficiency leads to stem cell factor-dependent clonal expansion of dysfunctional erythroid progenitors. Blood. 2018;132(22):2406-2417.
19. Li M, Liu D, Xue F, et al. Stage-specific dual function: EZH2 regulates human erythropoiesis by eliciting histone and non-histone methylation. Haematologica. 2023;
20. Liu L, Lu JY, Li F, et al. IDH1 fine-tunes cap-dependent translation initiation. J Mol Cell Biol. 2019;11(10):816-828.
21. Mei Y, Liu Y, Ji P. Understanding terminal erythropoiesis: An update on chromatin condensation, enucleation, and reticulocyte maturation. Blood Rev. 2021;46(100740.
22. Gonzalez-Menendez P, Romano M, Yan H, et al. An IDH1-vitamin C crosstalk drives human erythroid development by inhibiting pro-oxidant mitochondrial metabolism. Cell Rep. 2021;34(5):108723.
23. Gu Y, Yang R, Yang Y, et al. IDH1 mutation contributes to myeloid dysplasia in mice by disturbing heme biosynthesis and erythropoiesis. Blood. 2021;137(7):945-958.
24. Chung C, Sweha SR, Pratt D, et al. Integrated Metabolic and Epigenomic Reprograming by H3K27M Mutations in Diffuse Intrinsic Pontine Gliomas. Cancer Cell. 2020;38(3):334-349 e339.
25. Trakarnsanga K, Griffiths RE, Wilson MC, et al. An immortalized adult human erythroid line facilitates sustainable and scalable generation of functional red cells. Nat Commun. 2017;8(14750.
26. Karahoda B, Pardeshi L, Ulas M, et al. The KdmB-EcoA-RpdA-SntB chromatin complex binds regulatory genes and

coordinates fungal development with mycotoxin synthesis. Nucleic Acids Res. 2022;50(17):9797-9813.
27. Zheng Q, Maksimovic I, Upad A, David Y. Non-enzymatic covalent modifications: a new link between metabolism and epigenetics. Protein Cell. 2020;11(6):401-416.
28. Sun L, Zhang H, Gao P. Metabolic reprogramming and epigenetic modifications on the path to cancer. Protein Cell. 2022;13(12):877-919.
29. Grewal SI, Moazed D. Heterochromatin and epigenetic control of gene expression. Science. 2003;301(5634):798-802.
30. Goasguen JE, Bennett JM, Bain BJ, et al. Dyserythropoiesis in the diagnosis of the myelodysplastic syndromes and other myeloid neoplasms: problem areas. Br J Haematol. 2018;182(4):526-533.
31. Strahl BD, Allis CD. The language of covalent histone modifications. Nature. 2000;403(6765):41-45.
32. Tan M, Luo H, Lee S, et al. Identification of 67 histone marks and histone lysine crotonylation as a new type of histone modification. Cell. 2011;146(6):1016-1028.
33. Shah S, Henriksen MA. A novel disrupter of telomere silencing 1-like (DOT1L) interaction is required for signal transducer and activator of transcription 1 (STAT1)-activated gene expression. J Biol Chem. 2011;286(48):41195-41204.
34. Thomas GE, Egan G, Garcia-Prat L, et al. The metabolic enzyme hexokinase 2 localizes to the nucleus in AML and normal haematopoietic stem and progenitor cells to maintain stemness. Nat Cell Biol. 2022;24(6):872-884.
35. Gut P, Verdin E. The nexus of chromatin regulation and intermediary metabolism. Nature. 2013;502(7472):489-498.
36. Yego EC, Mohr S. siah-1 Protein is necessary for high glucose-induced glyceraldehyde-3-phosphate dehydrogenase nuclear accumulation and cell death in Muller cells. J Biol Chem. 2010;285(5):3181-3190.
37. Zhang T, Huang K, Zhu Y, et al. Vitamin C-dependent lysine demethylase 6 (KDM6)-mediated demethylation promotes a chromatin state that supports the endothelial-to-hematopoietic transition. J Biol Chem. 2019;294(37):13657-13670.
38. Mingay M, Chaturvedi A, Bilenky M, et al. Vitamin C-induced epigenomic remodelling in IDH1 mutant acute myeloid leukaemia. Leukemia. 2018;32(1):11-20.
39. Palis J. Ontogeny of erythropoiesis. Curr Opin Hematol. 2008;15(3):155-161.
40. Hattangadi SM, Martinez-Morilla S, Patterson HC, et al. Histones to the cytosol: exportin 7 is essential for normal terminal erythroid nuclear maturation. Blood. 2014;124(12):1931-1940.
41. Godfrey L, Crump NT, OByrne S, et al. H3K79me2/3 controls enhancer -promoter interactions and activation of the pan-cancer stem cell marker PROM1/CD133 in MLL-AF4 leukemia cells. Leukemia. 2021;35(1):90-106.
42. Godfrey L, Crump NT, Thorne R, et al. DOT1L inhibition reveals a distinct subset of enhancers dependent on H3K79 methylation. Nat Commun. 2019;10(1):2803.
43. Li T, Liu Q, Garza N, Kornblau S, Jin VX. Integrative analysis reveals functional and regulatory roles of H3K79me2 in mediating alternative splicing. Genome Med. 2018;10(1):30.
44. Kuno A, Hosoda R, Tsukamoto M, et al. SIRT1 in the cardiomyocyte counteracts doxorubicin-induced cardiotoxicity via regulating histone H2AX. Cardiovasc Res. 2022;
45. Liu Y, Shi G. Roles of sirtuins in asthma. Respir Res. 2022;23(1):251.
46. Zhang W, Zhou X, Hou W, et al. Reversing the imbalance in bone homeostasis via sustained release of SIRT-1 agonist to promote bone healing under osteoporotic condition. Bioact Mater. 2023;19(429-443.
47. Rajendran R, Garva R, Krstic-Demonacos M, Demonacos C. Sirtuins: molecular traffic lights in the crossroad of oxidative stress, chromatin remodeling, and transcription. J Biomed Biotechnol. 2011;2011(368276.
48. Dai Y, Chen T, Ijaz H, Cho EH, Steinberg MH. SIRT1 activates the expression of fetal hemoglobin genes. Am J Hematol. 2017;92(11):1177-1186.
49. Li L, Osdal T, Ho Y, et al. SIRT1 activation by a c-MYC oncogenic network promotes the maintenance and drug resistance of human FLT3-ITD acute myeloid leukemia stem cells. Cell Stem Cell. 2014;15(4):431-446.

50. Huang FT, Sun J, Zhang L, et al. Role of SIRT1 in hematologic malignancies. J Zhejiang Univ Sci B. 2019;20(5):391-398.

FIGURE LEGENDS

Figure 1. IDH1 deficiency impaired terminal stage erythropoiesis. (A) Representative cytospin images on proerythroblasts, basophilic erythroblasts, polychromatic erythroblasts, and orthochromatic erythroblasts differentiated from cord blood haematopoietic stem cells. The red arrows point to the cells that are abnormal nucleus. Scale bar, 10 μm. Quantitative analysis of the percentage of abnormal nuclear cells from three independent experiments. **(B)** Flow cytometry analysis showed the efficiency of enucleation on day 13 and day 15. Quantitative analysis of enucleation efficiency from three independent experiments. **(C)**Representative cytospin images of erythroblasts after adding GSH (50 μM) and NAC (10 μM) on day 15. Scale bar, 10 μm. Quantitative analysis of the percentage of the cells with abnormal nucleus. **(D)** Flow cytometry analysis showed the enucleation efficiency after adding GSH (50 μM) and NAC (10 μM) on day 15. Quantitative analysis of the enucleation efficiency after adding GSH (50 μM) and NAC (10 μM) on day 15 from three independent experiments. **(E)**Representative cytospin images of erythroblasts after supplement α-KG (50 μM) on day 15. Scale bar, 10 μm. Quantitative analysis of the percentage of the abnormal nucleus from three independent experiments. **(F)**Flow cytometry analysis showed the efficiency of enucleation after supplement α-KG (50 μM) on day 15. Quantitative analysis of the enucleation efficiency after supplement α-KG (50 μM) on day 15 from three independent experiments. Statistical analysis is from three independent experiments, and the bar plot represents mean ± SD of triplicate samples. Not significant (ns), * $p < 0.05$, ** $p < 0.01$, *** $p < 0.001$.

Figure 2. IDH1 localizes to nucleus in human erythroid cells. (A-B) Nuclear location of IDH1 (green) on the terminal stages of erythroid cells. Normal human terminal erythroid cells induced from umbilical cord blood-derived $CD34^+$ cells were stained with antibodies targeting IDH1 together with GPA (red) and Hoechst 33342 (blue). Scale bars, 5μm. MFI (mean fluorescent intensity) of IDH1 in nucleus and cytoplasm during the terminal stages of erythropoiesis was shown at the lower panel. **(C)** Representative immunofluorescence images showed the location of IDH1 at different time points in the human umbilical cord blood-derived erythroid progenitor 2 (HUDEP-2) cell line. IDH1 (green), GPA (red) and Hoechst 33342 (blue). Scale bars, 5μm. MFI of IDH1 in nucleus and cytoplasm of erythroid cells was shown at right panel. Data are presented as the mean ± SD from three independent experiments containing at least 30 cells each. **(D)** Representative immunofluorescence images of IDH1 (green), GPA (red) and Hoechst 33342 (blue) staining of the paraffin-embedded human bone marrow

cells of AML and MDS patients with IDH1 mutation. a. AML1, b. MDS-EB1. Scale bars, 5μm. **(E)** Representative immunofluorescence images of IDH1 (green), GPA (red) and Hoechst 33342 (blue) staining of the 293T cells. Scale bars, 5μm. **(F)** Representative western blotting images showed the protein expression level of IDH1 on nucleus and cytoplasm of terminal erythroid cells, 293T cells, human HUDEP2 cell lines, K562 and HEL cell lines. RCC1 was used as nuclear loading control, while Tubulin was used as cytoplasm loading control.

Figure 3. Nuclear IDH1 deletion increased abnormal nuclear cells.

(A) Schematic diagram of selectively knockdown nuclear IDH1. **(B)** A working model for the construction of Sg-IDH1 HUDEP2 cell line and Sg-NES-IDH1 HUDEP2 cell line. **(C)** Representative immunofluorescence images of location of IDH1 at D8 in HUDEP-2 cell lines. IDH1 (purple), GPA (red) and Hoechst 33342 (blue). Scale bars, 5μm. **(D)** Representative western blotting images showed the expression level of IDH1 at D8 in the HUDEP-2 cell lines. **(E)** Representative cytospin images of control, Sg-IDH1 HUDEP2 cell line and Sg-NES-IDH1 HUDEP2 cell line. Scale bars, 5μm. **(F)** Quantitative analysis of the percentage of the abnormal nucleus.Statistical analysis is from 3 independent experiments, and the bar plot represents mean ± SD of triplicate samples. Not significant (ns), * $p < 0.05$, ** $p < 0.01$, *** $p < 0.001$.

Figure 4. Deficiency of IDH1 reshape chromatin landscape. **(A)** Representative western blotting images showed the expression level of IDH1 in nucleus, chromatin and cytoplasm of erythroid cells cultured on day 15. **(B)** Representative transmission electron microscopy images showed the distribution of euchromatin and heterochromatin in nuclear on day 15 erythroid cells. **(C)** Quantitative analysis showed the area ratio of euchromatin and heterochromatin from three independent experiments. **(D)** Representative immunofluorescence images of **(a)** H3K79me3 (green), **(b)** H3K9me3 (green), **(c)** H3K27me2 (green). GPA (red) and Hoechst 33342 (blue) staining of Luciferase-shRNA and IDH1-shRNA erythroid cells cultured on day 15. Scale bar, 10 μm. **(E)** Representative western blotting images showed the abundance of H3K79me3, H3K9me3, H3K27me2 in nucleus and cytoplasm of Luciferase-shRNA and IDH1-shRNA erythroid cells cultured on day 15. **(F)** Quantitative analysis of the abundance of H3K79me3, H3K9me3, H3K27me2 in nucleus (above) and cytoplasm (below) of Luciferase-shRNA and IDH1-shRNA erythroid cells cultured on day 15 from three independent experiments. The bar plot represents mean ± SD of triplicate samples. Not significant (ns), * $p < 0.05$, ** $p < 0.01$, *** $p < 0.001$.

Figure 5. Identification of H3K79me3 as the critical factor in response to IDH1 deficiency. (A) Heatmaps displayed normalized ChIP signal of H3K27me2 (left), H3K79me3 (middle), and H3K9me3 (right) at gene body regions. The window represents ±1.5 kb regions from the gene body. TES, transcriptional end site; TSS, transcriptional start site. **(B)** Representative peaks chart image showed normalized ChIP signal of H3K27me2 (cyan), H3K79me3 (blue), and H3K9me3 (yellow) at gene body regions. **(C)** Statistics analysis of total peak number of H3K27me2, H3K79me3, and H3K9me3. **(D)** The bar plot showed the distribution of ChIPseeker-derived annotations of the genomic loci covered by peaks of H3K79me3, H3K27me2, and H3K9me3. **(E)** Statistics analysis of promoter peak number of H3K27me2, H3K79me3, and H3K9me3. **(F)** The bar plot showed GO enrichment analysis of the H3K79me3 peaks linked gene promoter.

Figure 6. IDH1 deletion increase the chromatin accessibility in late-stage erythroid cells. (A) Heatmaps displayed ATAC signal of Luciferase-shRNA (left) and IDH1-shRNA (right) at TSS. The window represents ±1.5 kb regions from the TSS. **(B)** Representative peaks chart image showed ATAC signal of IDH1-shRNA (green) and Luciferase-shRNA (blue) at TSS. **(C)** The volcano map showed differentially accessible peaks of gain (red color) and loss (blue color). **(D)** The bar plot displayed the distribution of peaks relative to gene features for differentially accessible peaks. **(E)** The bar plot showed GO enrichment analysis of the gained peaks linked gene promoter. **(F)** The top regulatory protein-binding sites identified by the HOMER algorithm from differentially accessible peaks. The top 10 motifs were ranked by p value.

Figure 7. Integrated analysis of ChIP-seq, ATAC-seq and RNA-seq. (A) GSEA analysis showed chromatin associated pathways from DEGs with promoter region marked by H3K79me3. **(B)** Gene overlap analysis of ATAC-seq, ChIP-seq and RNA-seq. **(C)** Chromatin associated genes overlap analysis of ATAC-seq, ChIP-seq and RNA-seq. **(D)** *SIRT1, KMT5A and NUCKS1* gene locus. Patterns of H3K79me3 modification denoted by ChIP peaks (red) are apparent in IDH1-shRNA increased chromatin accessibility (identified by ATAC-seq) (orange) and gene expression (identified by RNA-seq) (blue). **(E)** KLF1 binding sites of *SIRT1, KMT5A and NUCKS1* locus. **(F)** DNA pull-down assay showed KLF1 and H3K79me3 could binding to *SIRT1* gene promoter.

Figure 8. SIRT1 plays a critical role in mediating the regulatory effect of IDH1 during terminal stage erythropoiesis. **(A)** Representative cytospin images of Normal-SRT1720 (0 nM, 100 nM, 500 nM, 2.5 μM) on day 13 and day 15. The red arrows point to the cells with abnormal nucleus. Scale bar,

10 μm. Statistics analysis of abnormal nuclear cells from three independent experiments. **(B)** Flow cytometric showing the enucleation efficiency of Normal-SRT1720 (0 nM, 100 nM, 500 nM, 2.5 μM) on day 13 and day 15. Statistics analysis of enucleation efficiency from three independent experiments. **(C)** Representative cytospin images of Luciferase-shRNA, IDH1-shRNA, IDH1-shRNA-EX527 (10 nM, 200 nM) on day 13 and day 15. The red arrows point to the cells that are abnormal nucleus. Scale bar, 10 μm.Statistics analysis of abnormal nuclear cells from three independent experiments. **(D)** Flow cytometric showing the enucleation efficiency of Luciferase-shRNA, IDH1-shRNA, IDH1-shRNA-EX527 (10 nM, 200 nM) on day 13 and day 15. Statistics analysis of enucleation efficiency from three independent experiments. Statistical analysis is from three independent experiments, and the bar plot represents mean ± SD of triplicate samples. Not significant (ns), * $p < 0.05$, ** $p < 0.01$, *** $p < 0.001$.

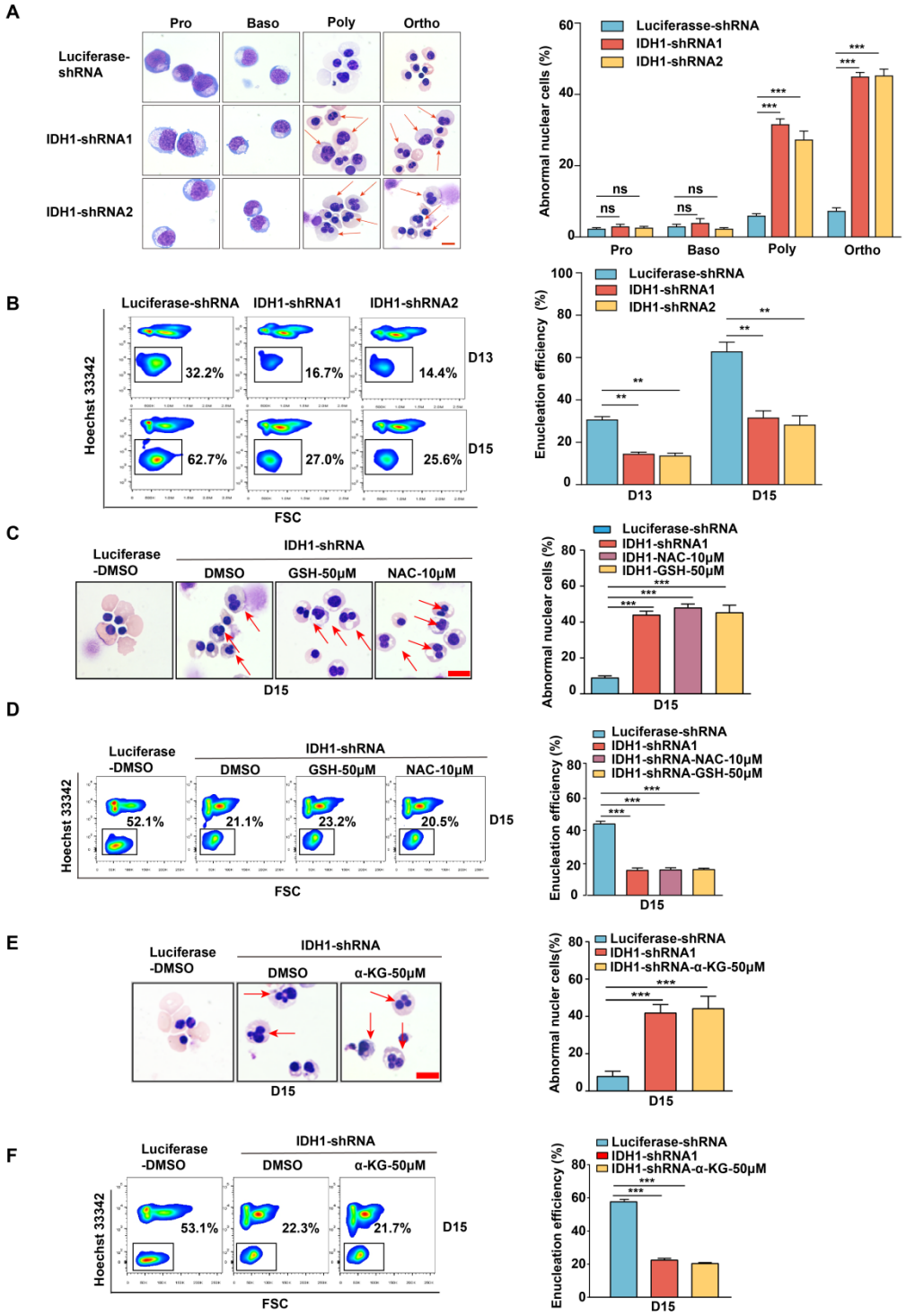

Figure 1. IDH1 deficiency impaired terminal stage erythropoiesis.

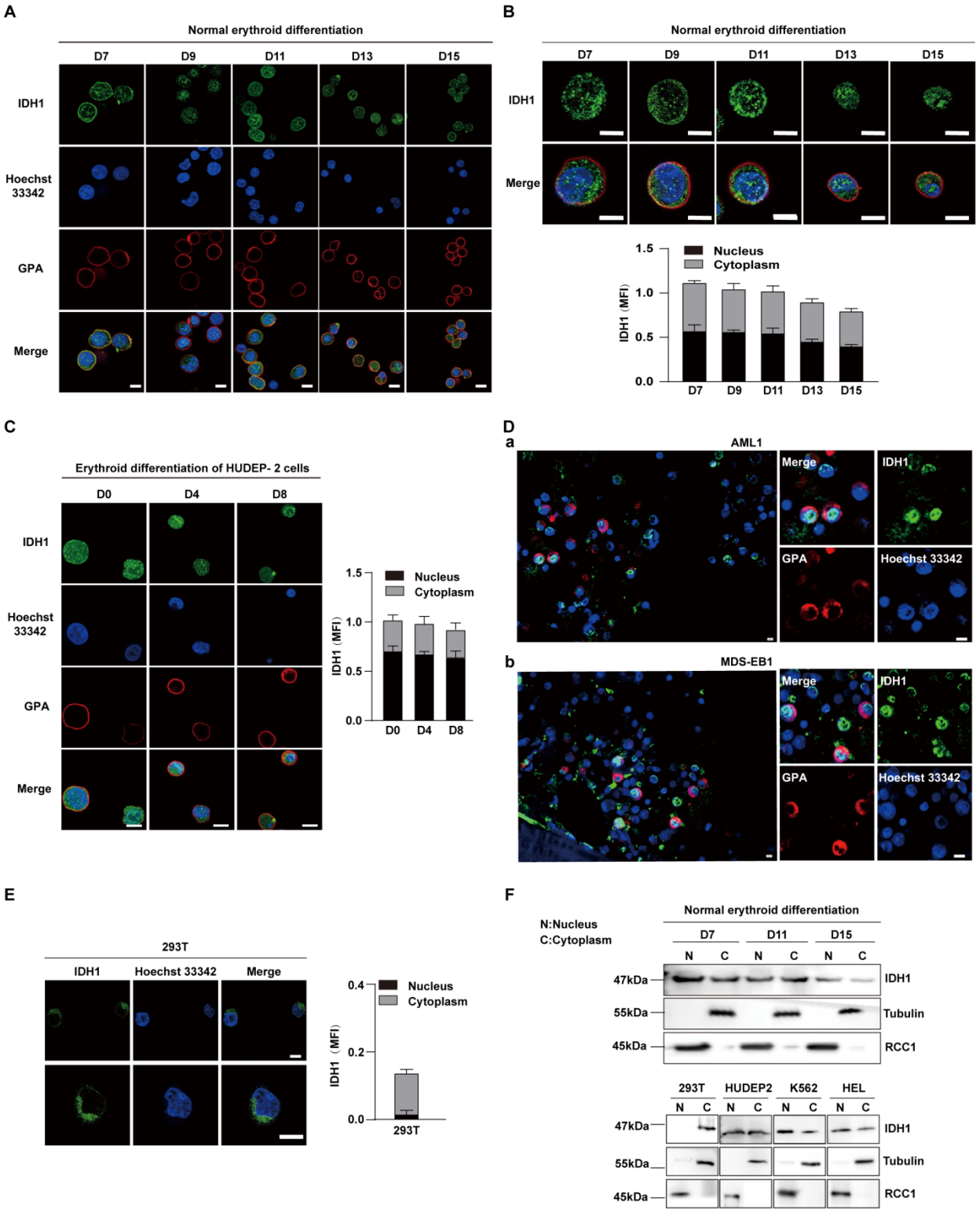

Figure 2. IDH1 localizes to nucleus in human erythroid cells.

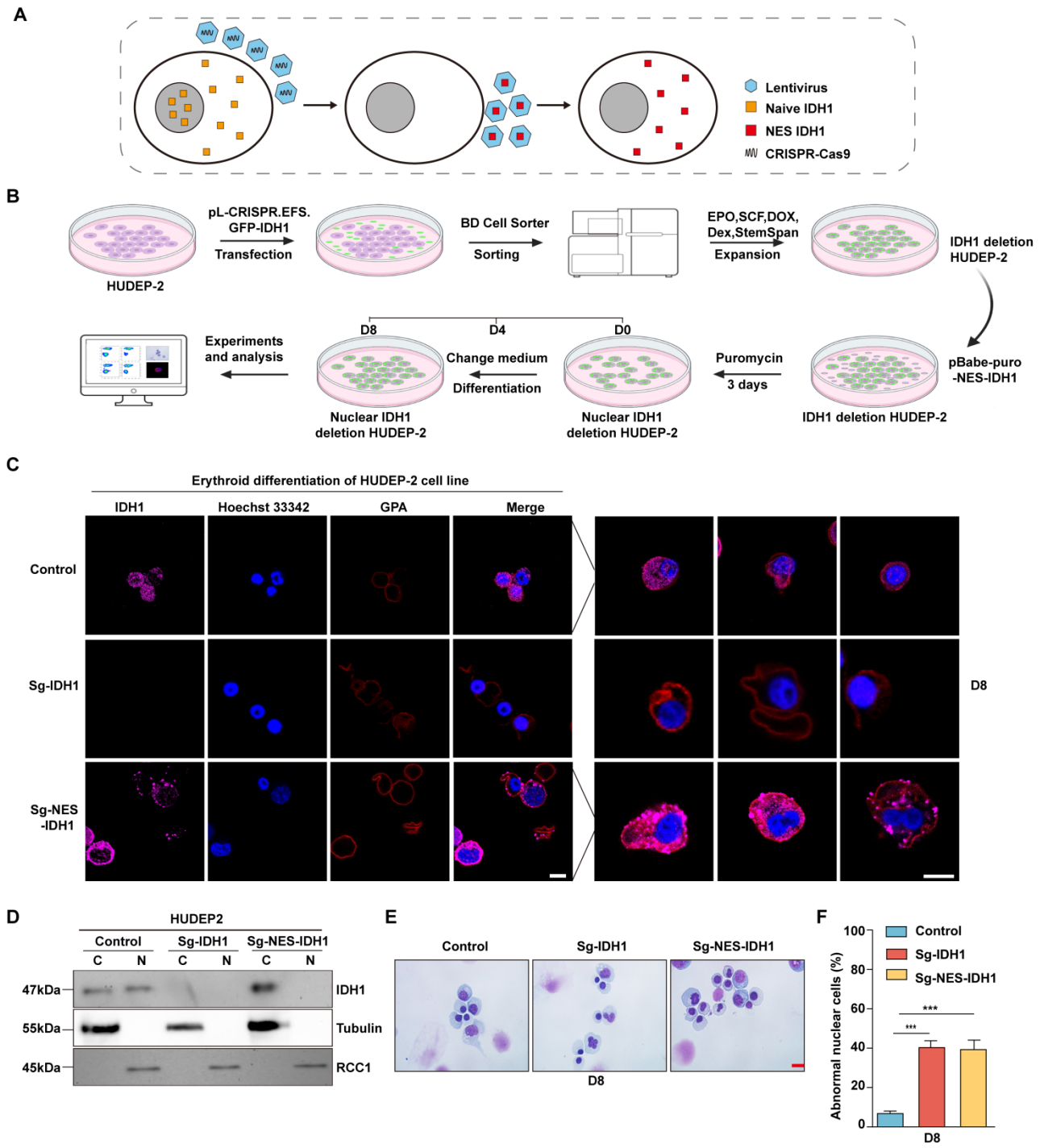

Figure 3. Nuclear IDH1 deletion increased abnormal nuclear cells.

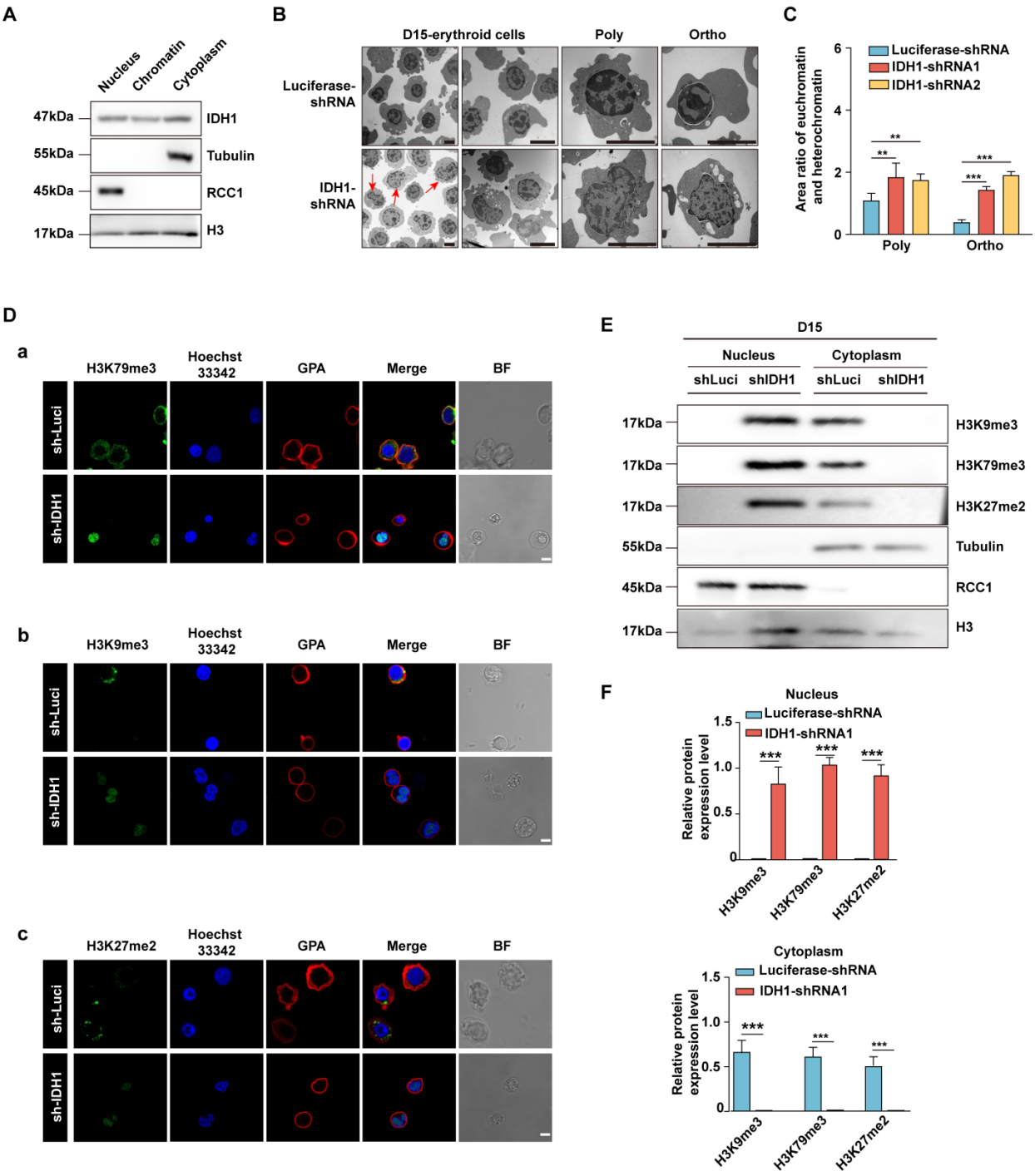

Figure 4. Deficiency of IDH1 reshape chromatin landscape.

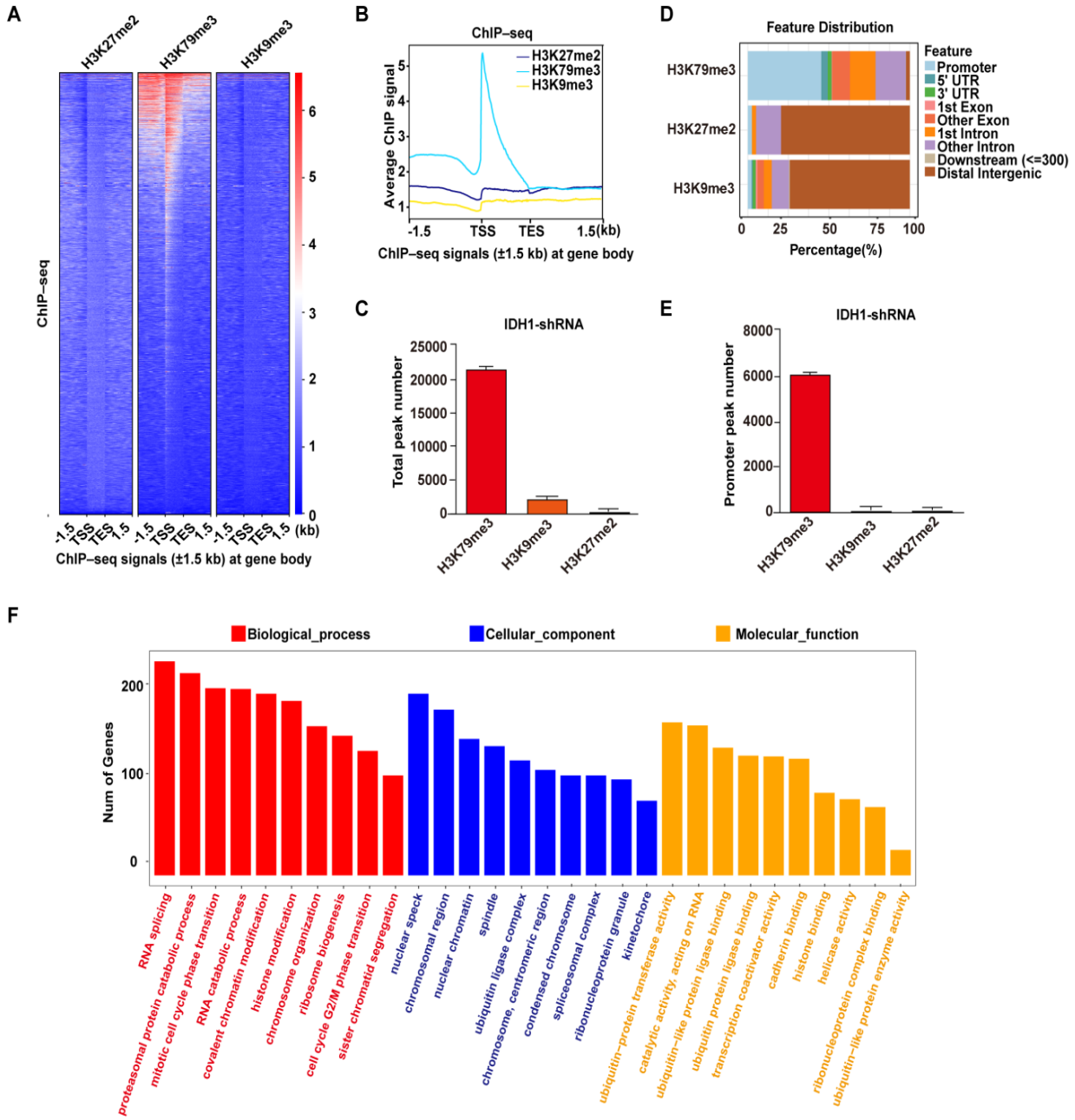

Figure 5. Identification of H3K79me3 as the critical factor in response to IDH1 deficiency.

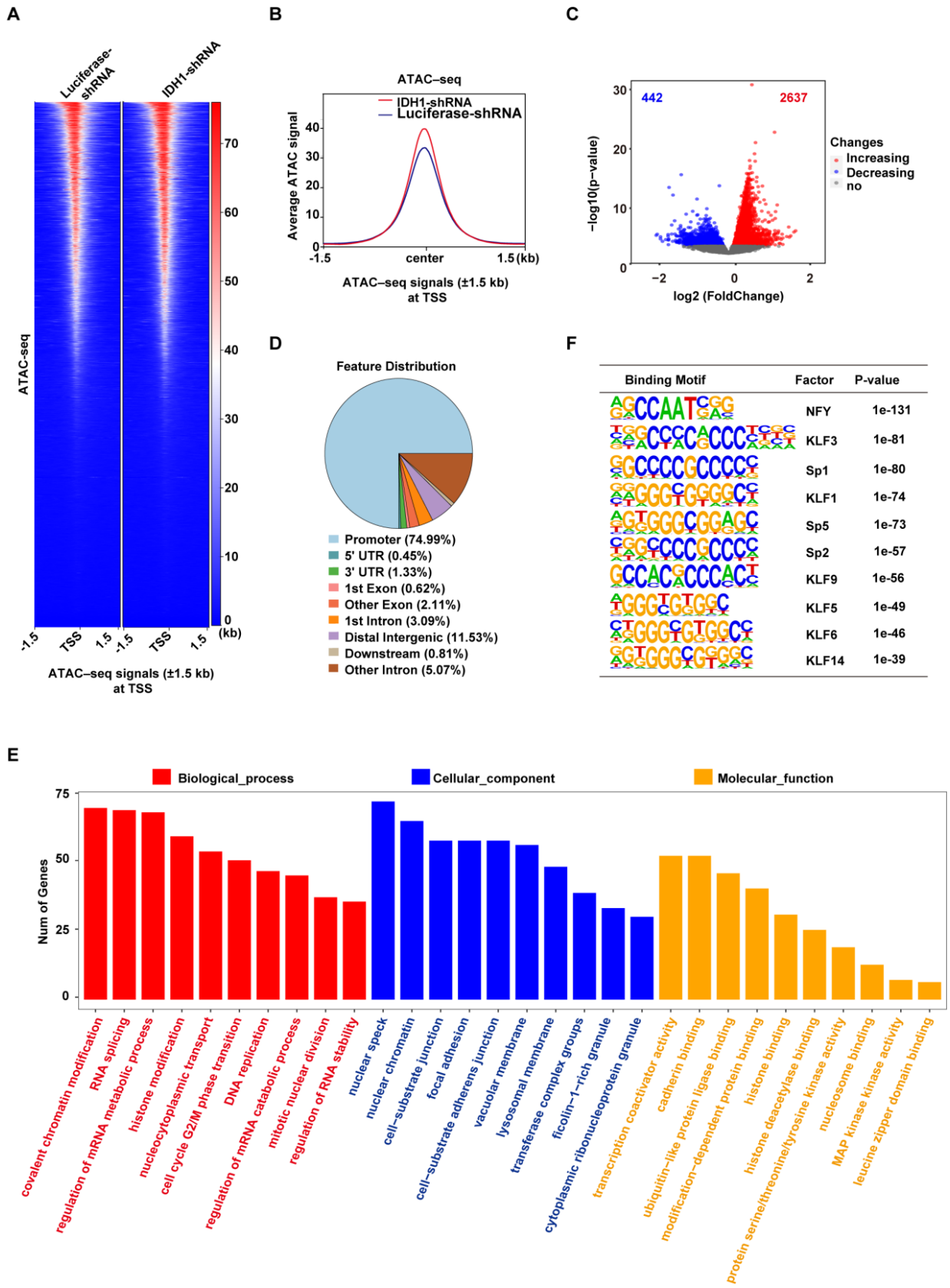

Figure 6. IDH1 deletion increase the chromatin accessibility in late-stage erythroid cells.

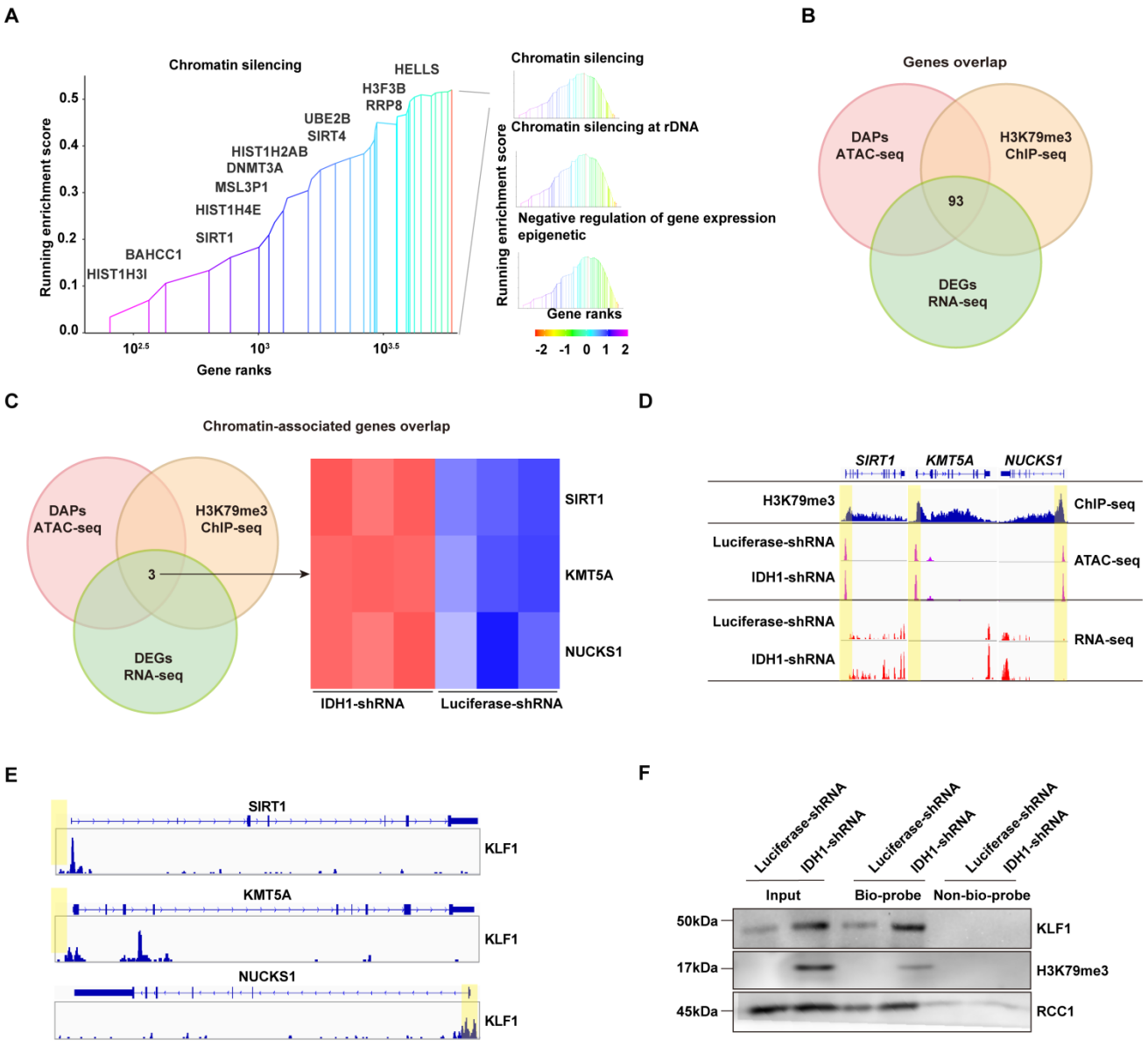

Figure 7. Integrated analysis of ChIP-seq, ATAC-seq and RNA-seq.

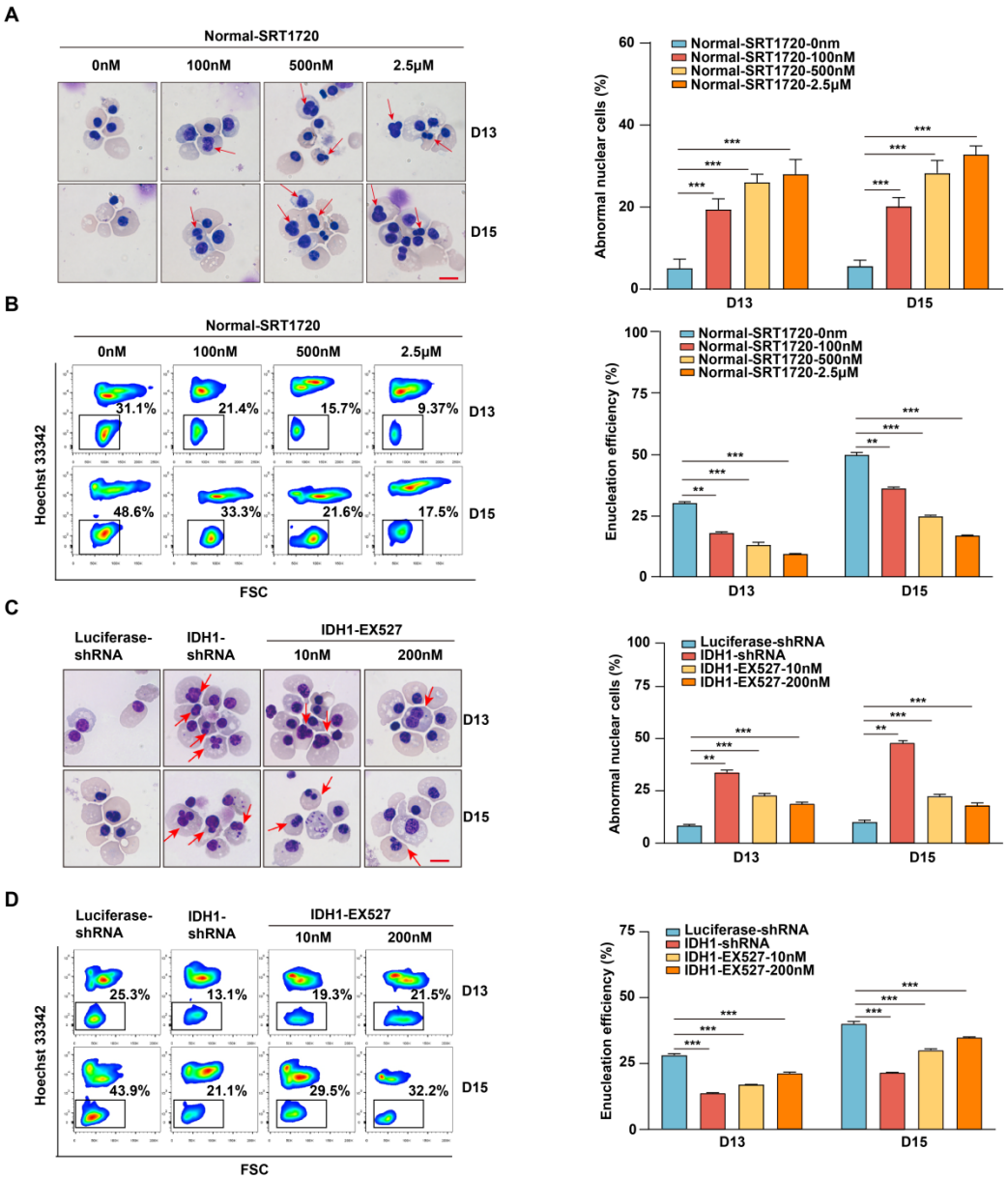

Figure 8. SIRT1 plays a critical role in mediating the regulatory effect of IDH1 during terminal stage erythropoiesis.